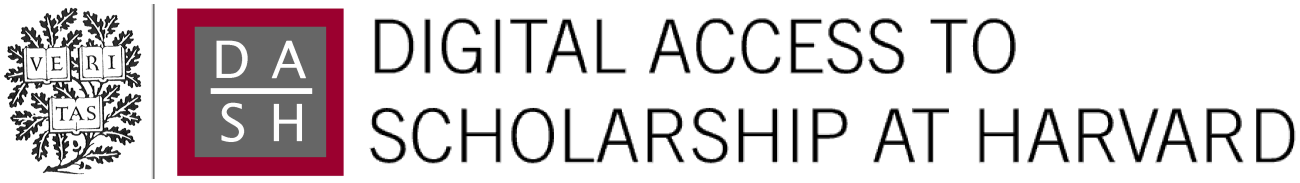

Reduced Caudate and Nucleus Accumbens Response to Rewards in Unmedicated Subjects with Major Depressive Disorder

Supplemental Material

Manuscript Title: Reduced Caudate and Nucleus Accumbens Response to Rewards in Unmedicated Subjects with Major Depressive Disorder

Authors: Diego A. Pizzagalli, Avram J. Holmes, Daniel G. Dillon, Elena L. Goetz, Jeffrey L. Birk, Ryan Bogdan, Darin D. Dougherty, Dan V. Iosifescu, Scott L. Rauch, Maurizio Fava

Methods

Individual titration and optimization of monetary incentive delay task

To increase the believability of the feedback manipulation, the target presentation duration was varied across successful trials (gains on reward trials, no-change on loss trials) and unsuccessful trials (no-change on reward trials, penalties on loss trials). To this end, prior to fMRI collection, participants completed 40 practice trials. For each subject, the 85th and 15th percentiles of the reaction time distribution during practice were used as the target durations on successful and unsuccessful trials, respectively. Because participants were instructed that the outcome of a trial depended on how fast they pressed a button after the appearance of the target, this manipulation served to justify outcome delivery (e.g., unsuccessful outcomes were associated with short target durations to which participants would have difficulty responding to quickly enough). Finally, to maximize task engagement, participants were instructed that good performance would yield an opportunity to play a sixth bonus block associated with increased gains ($3.63-$5.18) and infrequent penalties. Every participant "qualified" for the bonus block.

This combination of instructions and task design has been shown to lead to sustained task engagement and robust recruitment of brain reward circuitry (S1). Throughout the task, no information regarding cumulative earnings was provided.

The trial sequence was determined using Optseq (http://surfer.nmr.mgh.harvard.edu/optseq/) to optimize de-convolution of the hemodynamic response (S2). In addition, inter-stimulus interval and inter-trial interval durations were selected using a genetic algorithm to maximize the statistical orthogonality of the design and optimize estimation of hemodynamic responses (S3).

Functional and structural MRI data collection

Functional data were collected with z-shimming and a tilted slice acquisition (30^{o} from the AC-PC line). This sequence has been shown to increase signal recovery in the orbitofrontal cortex and medial temporal lobes without compromising temporal resolution or overall coverage (S1, S4). Data from the sixth "bonus" block were collected using non-optimized acquisition parameters to assess signal recovery in the behavioral blocks of interest, and are not included in the present analyses. Head movement was minimized with padding.

Methods and quality control of the MRI segmentation procedure

Structural labeling of the basal ganglia was achieved using FreeSurfer's subcortical segmentation procedure (S5), which was run along with the accompanying cortical parcellation algorithms (S6). FreeSurfer's segmentation processes work by incorporating information about the image intensity of different tissue classes with probabilistic information about the relative location of different brain regions, such that each voxel in a participant's structural image is

assigned a neuroanatomical label (S5, S7). Importantly, the probabilistic information is derived from a training data set that was manually labeled using validated techniques developed by the Center for Morphometric Analysis at Massachusetts General Hospital (e.g., S8, S9). Although FreeSurfer's steps can be run in fully automated mode and are designed to permit segmentation of very large numbers of brains per day (S5), in the present study they were run in stages and quality control was implemented at three separate points. The first set of quality controls involved checking that: (1) the participant's T1 image was correctly cross-registered to the MNI305 atlas in Talairach space (to increase the reliability of the probabilistic labeling); (2) a skull stripping procedure used to remove the skull and dura from the image was completed correctly; and (3) intensity normalization of the images was correct such that subsequent intensity-based segmentation steps would be accurate. Problems were rarely detected at any of the quality control points, but they were most frequent at this point and usually consisted of an inaccurate cross-registration and/or incomplete stripping of dura or eyes from around the orbitofrontal cortex. These problems were manually corrected by the second and third authors and the first stage was re-run and re-checked afterwards. The second set of quality controls was done to confirm that: (1) outlines of the pial and white matter surfaces of the brain were correctly drawn; (2) segmentation of white matter was accurate; and (3) the subcortical segmentation—including the segmentation of basal ganglia structures—was complete. Problems at this stage were generally minor and involved small errors in the pial and white matter surfaces (e.g., dura included in the pial surface, incomplete coverage of white matter in the superior temporal lobes). Again, these problems were manually corrected and the stage was re-run and re-checked afterwards. The final set of quality controls consisted of inspection of inflated cortical surfaces

and accompanying cortical parcellations (S6). Errors were very rarely detected at this stage, probably due to the careful checks implemented at points one and two.

Comparisons between manual and automatic anatomical tracings

Findings emerging from recent studies indicate that FreeSurfer's automated approach provides segmentation accuracy comparable to expert manual labeling. For the caudate (i.e., the region emerging from the current study as being significantly related to anhedonic symptoms), the percent spatial overlap between manual and automated tracings in prior studies ranged from satisfactory (0.76: S10) to excellent (>0.85; S5; 0.88: S11). Moreover, the test-retest reliability of FreeSurfer's dorsal striatum volume in a prior study was excellent (0.96; S12).

Of particular relevance to the current study, the Center for Morphometrical Analysis (Massachusetts General Hospital, Boston, MA) recently performed a comparison between FreeSurfer automatic tracing and manual tracing methods of the basal ganglia for a sample of 20 adults recruited from the community (age: 26.72±4.83, 11 females, 75% Caucasian). Data were collected at the same neuroimaging facility and using a similar MPRAGE acquisition protocol (TR/TE: 2530/3.30 voxel dimensions: 1.33 mm^3; flip angle = 7 degrees) as done in the current study. Before tracing, structural data were motion-corrected. As shown in Table S1, Pearson's correlations between the manual and automatic tracing methods were highly significant for the regions emerging from the current study (caudate, putamen, nucleus accumbens). With the exception of the left nucleus accumbens (r=0.556) all correlations exceeded r=0.78 (courtesy of Dr. Nikos Makris, Center for Morphometric Analysis, Massachusetts General Hospital, Boston, MA).

Correction for multiple comparisons using Monte Carlo simulations

In addition to evaluating results using the voxel and extent thresholds reported in the main text ($p<.005$, 12 voxels), between-groups differences in the contrast of primary interest (gains - no change feedback) were examined following correction for multiple comparisons using Monte Carlo simulations (mri_glmfit program in FS-FAST). To this end, the fMRI data for each subject was replaced with white Gaussian noise that was spatially smoothed to the same degree as the fMRI data, as measured from the residuals from the group analysis. The full analysis was then performed on this synthetic data set. Clusters were defined as connected sets of voxels whose p-values were less than 0.005 (the voxel-wise threshold). This was repeated 10,000 times to empirically determine the null distribution of the largest cluster size under our experimental conditions. This distribution was then used to compute the p-values of the clusters when the real data were analyzed.

Given our a priori interest in basal ganglia reward responses, the simulation only considered the basal ganglia. A mask of the four basal ganglia regions of interest (nucleus accumbens, caudate, putamen, pallidus) was generated by running the FreeSurfer subcortical segmentation on the high resolution "Collins" brain and then transforming the mask to Talairach space, and the Monte Carlo simulation was restricted to this mask volume. Accordingly, the results of this simulation were used only to determine the significance of findings in basal ganglia regions.

Results

Target Presentation Duration

MDD and comparison subjects had very similar 15th and 85th percentile reaction time values during practice, which were used to set target durations on unsuccessful and successful trials, respectively, during the experimental blocks (15th: 270.43±42.55 ms vs. 272.32±27.24 ms, t=-0.21, df=59, p>0.83; 85th: 370.27±66.46 ms vs. 385.52±83.72 ms; t=-0.79, df=59, p>0.43). In addition, analyses of reaction times collected during fMRI scanning revealed no main effects of *Group* (F=0.17, df=1,59, p>0.68; see Main Text), due to comparable overall reaction times in comparison 350.38±68.91) and MDD (357.01±75.60) subjects.

General performance in the Monetary Incentive Delay task

To further evaluate possible group differences in task difficulty, we computed (1) the percentage of reward trials ending in gains, (2) the percentage of loss trials ending in penalties, (3) the total number of errors committed (e.g., pressing the button in response to the cue instead of the target), and (4) the total money won, lost, and earned (i.e., won minus lost). As summarized in Table S2, no group differences emerged. Collectively, analyses of both reaction time and "accuracy" data collected during both the practice and imaging session suggest that fMRI findings were not confounded by group differences in task difficulty.

Affective ratings

Anticipation phase. Due to technical problems, the valence ratings for reward cues were lost for one comparison subject. The ANOVA revealed a main effect of *Group* (F=5.62, df=1,58, p<0.021) due to overall reduced positive affect in MDD versus comparison subjects (2.78±0.57

vs. 3.08±0.42) (Figure S1, panel A). The *Group* x *Cue* interaction was not significant (F=1.54, df=2,116, p>0.22). A trend for a main effect of *Cue* also emerged (F=2.99, df=2,116, p<0.054), due to significantly more positive valence ratings for the reward (3.07±0.87) versus loss cue (2.77±0.79; p<0.035).

For arousal ratings, the ANOVA revealed a main effect of *Cue* (F=4.50, df=2,118, p<0.013), due to increased arousal in response to both reward (3.05±0.69; p<0.017) and loss (3.07±0.75; p<0.015) cues relative to neutral cues (2.81±0.83). There was no difference in arousal elicited by reward and loss cues (p>0.84). Neither the main effect of *Group* (F=0.13, df=1,59, p>0.71) nor the *Group* x *Cue* interaction (F=2.32, df=2,118, p>0.10) was significant (Figure S1, panel B).

Outcome phase. For valence ratings, there was a main effect of *Group* (F=12.26, df=1,59, p<0.001) due to significantly less positive ratings in MDD than comparison subjects (2.79±0.44 vs. 3.16±0.38) (Figure S1, panel C). The *Group x Outcome* interaction was not significant (F=1.38, df=2,118, p>0.25). Additionally, the main effect of *Outcome* was significant (F=191.57, df=2,118, p<0.0001). As expected, gains elicited significantly more positive ratings (4.16±0.77) than penalties (1.80±0.82; p<0.0001) or no-change feedback (2.97±.47; p<0.0001). Moreover, penalties were rated as significantly more negative than no-change feedback (p<0.0001).

For arousal ratings, the ANOVA revealed a main effect of *Outcome* (F=9.02, df=2,118, p<0.0005) that was qualified by a significant *Group* x *Outcome* interaction (F=3.20, df=2,118, p<0.045). The main effect of *Group* was not significant (F=0.24, df=1,59, p>0.87). The *Outcome* effect reflected the fact that gains elicited significantly greater arousal (3.48±0.85) than penalty (3.08±1.13; p<0.015) or no-change feedback (2.87±0.89; p<0.0001), which did not differ from each other (p>0.15). Critically, however, relative to comparison subjects, MDD subjects reported

significantly less arousal in response to gains ($p<0.045$) but not penalties or no-change feedback ($ps>0.42$) (Figure S1, panel D). Moreover, within-group follow-up analyses indicated a lack of modulation for MDD subjects ($ps>0.16$). For comparison subjects, on the other hand, gains elicited significantly more arousal (3.69±0.79) than penalties (2.97±1.12; $p<0.0002$) or no-change feedback (2.81±0.75; $p<0.0002$). Collectively, these results show that cue and outcome stimuli generally elicited the intended affective responses, and indicate that MDD subjects experienced less positive affect during the anticipatory and consummatory phases of the task. Moreover, after receiving gains, MDD subjects reported less intense affective responses.

Secondary fMRI findings

Complete lists of regions showing group differences during incentive anticipation and consummation are presented in Tables S3 and S4, respectively.

Reward Anticipation (Reward cue – No-incentive cue). As described in the main text, relative to comparison subjects, MDD subjects showed relatively weaker activation to reward cues in the left posterior putamen. To further investigate this finding, a *Group* x *Cue* (reward, loss, no-incentive) ANOVA on beta weights extracted from this region was performed. The only significant finding was the *Group* x *Cue* interaction ($F=5.10$, $df=2,110$, $p<0.008$). Follow-up tests revealed that, for comparison subjects, both reward (mean=0.032±0.08; $p<0.005$) and loss (mean=0.031±0.06; $p<0.007$) cues elicited stronger activation compared to the no-incentive cue (mean=-0.019±0.08). For MDD subjects, on the other hand, reward cues (mean=-0.002±0.10), loss cues (mean=0.021±0.08), and no-incentive cues (mean=0.022±0.07) elicited similar responses, and no cue-related modulation was observed ($ps>0.21$). Follow-up tests revealed that groups differed in their responses to no-incentive ($p<0.05$) but not reward ($0>.15$) or loss

(p>0.60) cues. However a between-groups *t*-test of the reward minus no-incentive cue difference was also significant, $t(55) = -2.96$, $p = .005$, directly confirming the whole-brain result (comparison: mean=0.050±0.09; MDD: mean=-0.024±0.10).

Relative to comparison subjects, MDD subjects were characterized by significantly increased bilateral activation in various dorsolateral prefrontal cortex regions encompassing the middle and inferior frontal gyri (Figure S2). For the bilateral clusters (x=24, y=22, z=40; x=-28, y=24, z=40), beta weights were extracted and entered in a *Group* x *Hemisphere* x *Condition* ANOVA. The only significant finding was the *Group* x *Condition* interaction (F=11.00, df=2,110, p<0.0001). Follow-up analyses indicated that, relative to comparison subjects, MDD subjects had significantly greater bilateral dorsolateral prefrontal activation to reward (p<0.009) but not loss (p>0.78) or no-incentive (p>0.16) cues (Figure S2). Within-group analyses revealed that comparison subjects were characterized by significantly reduced activation in response to reward relative to no-incentive cues (p<0.015). MDD subjects, on the other hand, showed significantly greater activation in response to reward cues compared to both loss (p<0.025) and no-incentive (p<0.005) cues. The remaining two prefrontal clusters (left inferior frontal gyrus: x=-46, y=16, and z=28; right middle frontal gyrus: x=30, y=26, z=29) showed similar patterns.

Reward Outcomes (Gains – No-change feedback). In addition to showing a weaker striatal response to gains relative to comparison subjects, the MDD group also showed significantly weaker activation in the dorsal anterior cingulate cortex (x=10, y=18, z=30; Figure S3), a region that has been implicated in integrating reinforcement history over time (S13-S16). Analysis of beta weights (gains, penalties, no-change feedback) extracted from the dorsal anterior cingulate cortex revealed a significant *Group* x *Condition* interaction (F=6.61, df=2,110, p<0.002), due to a significant between-group difference (comparison > MDD) for gains

($p<0.001$) but not penalty or no-change feedback ($ps<0.42$). Whereas comparison subjects showed significantly greater cingulate activation in response to gains versus no-change feedback ($p<0.015$), MDD subjects showed a significantly weaker response to gains compared to both penalties and no-change feedback ($ps<0.05$; Figure S3).

Loss Anticipation (Loss cue – No-incentive cue). Relative to comparison subjects, MDD subjects showed significantly increased activation during anticipation of a potential loss in various regions, including the left insula (x=-38, y=-7, z=-6), right middle frontal gyrus (x=40, y=44, z=8), and dorsal anterior cingulate cortex (x=2, y=23, z=16) (Figure S4). Follow-up analyses indicated that MDD subjects activated these regions more strongly in response to loss (and reward) cues relative to no-incentive cues, whereas comparison subjects generally did not show any cue-specific modulation. These observations were corroborated by significant *Group* x *Condition* interactions for all three regions ($Fs>3.39$, df=2,110, $ps<0.045$); for the left insula and right middle frontal gyrus, the main effect of *Condition* was also significant ($Fs>6.64$, df=2,110, $ps<0.002$). Within-group analyses indicated that MDD subjects activated the left insula, right middle frontal gyrus, and dorsal anterior cingulate cortex more strongly in response to both loss and reward cues compared to the no-incentive cue (all $ps<0.009$; Figure S4). Comparison subjects, on the other hand, showed no condition-specific modulation in the right middle frontal gyrus or cingulate (all $ps>0.25$); for the left insula, comparison subjects showed significantly higher activation to the reward compared to loss cue ($p<0.015$). The only region showing significantly higher activation for comparison relative to MDD subjects was the cerebellum (Table S2).

Loss Outcomes (Penalties – No-change feedback). Relative to comparison subjects, the MDD group was characterized by significantly reduced activation in response to penalties in

various regions, including the bilateral caudate, thalamus, and right prefrontal cortex, among other regions (Table S3). For all these regions, including the left (x=-8, y=-2, z=12) and right (x=14, y=23, z=11) caudate, the ANOVA revealed significant *Group* x *Condition* interactions (Fs>3.17, df=2,110, ps<0.047) in the absence of *Group* main effects (Figure S5). Within-group analyses showed that comparison subjects activated both the left and right caudate significantly more to penalties (and gains) versus no-change feedback (ps<0.05), whereas MDD subjects showed no modulation (ps>0.15). Moreover, in this left caudate cluster, comparison subjects showed significantly higher activation than MDD subjects to penalties (p<0.015); there was no between-group difference in response to penalties in the right caudate. Relatively increased activation for MDD relative to comparison subjects was observed only in the right cerebellum and left precuneus.

Morphometical Basal Ganglia Data

The absolute and proportional volumes of single basal ganglia regions are listed in Table S5. The *Group* x *Hemisphere* x *Region* ANOVA revealed a significant main effect of *Structure* and a *Structure* x *Hemisphere* interaction, which were not explored further. The main effect of *Group* was not significant (F=0.73, df=1,59, p>0.35). The only other effect approaching significance was the *Group* x *Hemisphere* x *Structure* interaction (F=2.47, df=3,177, p=0.086, ε=0.67). However, follow-up analyses revealed no volumetric group differences (all ps>0.18).

Control analyses

Analyses comparing MDD subject with (N=14) vs. without (N=16) comorbid anxiety disorders. For the reaction time data, a *MDD Subgroup* (MDD with vs. without comorbid

anxiety disorder) x *Cue* ANOVA revealed no effects involving *MDD Subgroup* (Fs<0.40, ps>0.50). For the affective ratings, the only effects of interest were main effects of *MDD Subgroup* for the arousal ratings for both the anticipatory (F=8.57, df=1,28, p<0.008) and consummatory (F=7.83, df=1,28, p<0.009) phase, which were due to higher arousal rating for MDD subjects with comorbid anxiety relative to MDD subjects without anxiety comorbidity. No effects involving *MDD Subgroup* emerged for the left putamen (anticipatory phase), left nucleus accumbens (consummatory phase), or caudate (consummatory phase) clusters (all Fs<1.24, all ps>0.29).

Functional MRI findings adjusted for affective ratings. For the main regions-of-interest emerging from the whole-brain between-group analyses, hierarchical regression analyses were performed to evaluate whether differences remained after accounting for group differences in the affective ratings. For the left posterior putamen region implicated in reward anticipation, valence ratings in response to the reward cues were entered in the first step, whereas *Group* (dummy-coded) was entered in the second step. For the left nucleus accumbens and bilateral caudate regions emerging from the analyses of gains, valence and arousal ratings in response to gains were entered in the first step, and *Group* was entered in the second step (data from the caudate were first averaged across hemispheres). For all regions the model was significant, indicating that *Group* predicted differences in left putamen (ΔR^2=0.104), left nucleus accumbens (ΔR^2=0.094), and caudate (ΔR^2=0.187) activation above and beyond group differences in affective ratings (all ΔF>5.74, all ps<0.020).

Functional MRI findings adjusted for striatal volume. A second set of hierarchical regression analyses were performed to evaluate whether the group differences in left nucleus accumbens and bilateral caudate responses to gains remained after adjusting for proportional

volume. For both regions (left nucleus accumbens: ΔR^2=0.116; caudate: ΔR^2=0.243), *Group* predicted activation to gains after controlling for volume (all ΔF*s*>7.33, *p*s<0.009).

Functional MRI findings adjusted for reward-related reaction time modulation. A final set of hierarchical regression analyses were performed to evaluate whether the group differences in left nucleus accumbens and bilateral caudate responses to gains remained after adjusting for group differences in reward-related reaction time modulation (no-incentive – reward difference score). For both regions, *Group* uniquely predicted activation to gains after controlling for reaction time differences (left nucleus accumbens: ΔR^2=0.130; caudate: ΔR^2=0.212), (all ΔF*s*>8.10, *p*s<0.007).

Corrections for multiple comparisons using Monte Carlo simulations. Of the five basal ganglia clusters evident at p<.005, 12 voxel extent, three were significant at p<.05 following correction for multiple comparisons: both clusters in the right caudate and one in the left caudate (Table S4). The second cluster in the left caudate and the left nucleus accumbens cluster were not significant, p>.05, likely due to their smaller size.

Correlations between functional MRI and volumetric data. At the request of an anonymous reviewer, correlational analyses between functional and volumetric data were performed. To this end, beta weights in response to gains were extracted from structurally defined left nucleus accumbens and bilateral caudate regions. The mean beta weight across the entire structure was then correlated with the volume of the region. For both MDD and comparison subjects, no significant correlations emerged for either the nucleus accumbens (MDD: r=0.35, p>0.075; comparison: r=-0.03, p>0.88) or bilateral caudate (MDD: r=0.06, p>0.78; comparison: r=-0.09, p>0.65).

References

S1. Dillon DG, Holmes AJ, Jahn AL, Bogdan R, Wald LL, Pizzagalli DA: Dissociation of neural regions associated with anticipatory versus consummatory phases of incentive processing. Psychophysiology 2008; 45:36-49.

S2. Dale AM: Optimal experimental design for event-related fMRI. Hum Brain Mapp 1999; 8:109-114.

S3. Wager TD, Nichols TE: Optimization of experimental design in fMRI: a general framework using a genetic algorithm. NeuroImage 2003; 18:293-309.

S4. Deichmann R, Gottfried JA, Hutton C, Turner R: Optimized EPI for fMRI studies of the orbitofrontal cortex. NeuroImage 2003; 19:430-441.

S5. Fischl B, Salat DH, Busa E, Albert M, Dieterich M, Haselgrove C, van der Kouwe A, Killiany R, Kennedy D, Klaveness S, Montillo A, Makris N, Rosen B, Dale AM: Whole brain segmentation: automated labeling of neuroanatomical structures in the human brain. Neuron 2002; 33: 341-355.

S6. Fischl B, van der Kouwe A, Destrieux C, Halgren E, Segonne F, Salat DH, Busa E, Seidman LJ, Goldstein J, Kennedy D, Caviness V, Makris N, Rosen B, Dale A: Automatically parcellating the human cerebral cortex. Cereb Cortex 2004; 14: 11-22.

S7. Walhovd KB, Moe V, Slinning K, Due-Tønnessen P, Bjørnerud A, Dale AM, van der Kouwe A, Quinn BT, Kosofsky B, Greve D, Fischl B: Volumetric cerebral characteristics of children exposed to opiates and other substances in utero. NeuroImage 2007; 36: 1331-1344.

S8. Caviness VS Jr., Meyer J, Makris N, Kennedy DN: MRI-based topographic parcellation of the human neocortex: an anatomically specified method with estimate of reliability. J Cogn Neurosci 1996; 8: 566-587.

S9. Kennedy DN, Filipek PA, Caviness VS: Anatomic segmentation and volumetric calculations in nuclear magnetic resonance imaging. IEEE Transactions on Medical Imaging; 8: 1-7.

S10. Khan AR, Wang L, Beg MF: FreeSurfer-initiated fully-automated subcortical brain segmentation in MRI using Large Deformation Diffeomorphic Metric Mapping. NeuroImage; 41: 735-746.

S11. Han X, Fischl B: Atlas renormalization for improved brain MR image segmentation across scanner platforms. IEEE Trans Med Imaging 2007; 26: 479-486.

S12. Goldman AL, Pezawas L, Mattay VS, Fischl B, Verchinski BA, Zoltick B, Weinberger DR, Meyer-Lindenberg A: Heritability of brain morphology related to schizophrenia: a large-scale automated magnetic resonance imaging segmentation study. Biol Psychiatry 2008; 63: 475-483.

S13. Kennerley SW, Walton ME, Behrens TEJ, Buckley MJ, Rushworth, MFS: Optimal decision making and the anterior cingulate cortex. Nat Neurosci 2006; 9:940-947.

S14. Santesso DL, Dillon DG, Birk JL, Holmes AJ, Goetz E, Bogdan R, Pizzagalli DA: Individual differences in reinforcement learning: Behavioral, electrophysiological, and neuroimaging correlates. NeuroImage 2008; 42:807-816.

S15. Santesso DL, Evins AE, Frank MJ, Schetter CE, Pizzagalli DA: Single dose of a dopamine agonist impairs reinforcement learning in humans: Evidence from

electrophysiology and computational modeling of striatal-cortical function. Hum Brain Mapp, in press.

S16. Rushworth MF, Buckley MJ, Behrens TE, Walton, ME, Bannerman DM: Functional organization of the medial frontal cortex. Curr Opin Neurobiol 2007; 17:220-227.

Table S1: Summary of Pearson's correlations between basal ganglia volumes determined by FreeSurfer automatic tracing and manual tracing methods for a sample of 20 community adults (courtesy of Dr. Nikos Makris, Center for Morphometric Analysis, Massachusetts General Hospital, Boston, MA).

Basal Ganglia Volume	**Pearson r**	**p-value**
Right Caudate	0.880	0.0000003
Left Caudate	0.875	0.0000005
Right Putamen	0.932	0.0000001
Left Putamen	0.795	0.0000279
Right Accumbens	0.784	0.0000435
Left Accumbens	0.556	0.0108939

Table S2: Summary of task "performance" in the MID task.

	Comparison subjects	**MDD subjects**	**T statistic**	**p-value**
% Reward trials ending in gains	48.68 (1.76)	48.31 (1.91)	-0.76	0.45
% Loss trials ending in penalties	47.94 (2.68)	47.62 (2.86)	-0.44	0.67
Total number of errors	4.06 (3.92)	4.92 (4.81)	0.74	0.46
Total $ won	41.72 (1.59)	41.10 (2.46)	-1.14	0.26
Total $ lost	47.05 (6.50)	49.00 (9.16)	-0.91	0.37
Total $ earned	-5.13 (7.19)	-7.91 (9.93)	-1.22	0.23

Note: the overall net loss reflects the fact that while gains were slightly larger than penalties, participants were penalized $2 for each error. The sixth "bonus" block included three large gains ($3.68, $4.72, and $5.18) against one scheduled loss (-$1.53), so that most participants would experience a net gain. Each participant was paid $20-22 dollars for playing the game.

TABLE S3. Regions Showing Group Differences Between MDD (N=26) and Comparison Subjects (N=31) During the Anticipation of a Potential Reward or Loss

Region	*x*	*y*	*z*	Volume (mm^3)	Peak Voxel p-value
A. Reward Cue – No Incentive Cue					
Comparison Subjects > MDD					
L Putamen	-28	-13	-2	192	0.0001
R Occipitofrontal Fasciculus	30	-34	32	144	0.0010
R Middle Occipital Gyrus	38	-65	1	136	0.0002
MDD > Comparison Subjects					
R. Uncus/Parahippocampal gyrus	34	-2	-28	128	0.0011
R Inferior Frontal Gyrus	55	34	-3	504	0.0002
L Inferior Frontal Gyrus	-46	16	28	176	0.0012
R Middle Frontal Gyrus	24	22	40	432	0.0001
	30	26	29	304	0.0001
L Middle Frontal Gyrus	-28	24	40	480	0.0003
R. Subgenual Cingulate	12	32	-9	176	0.0004
R. Superior Temporal Gyrus	57	-10	5	120	0.0004
L. Occipitofrontal Fasciculus/Cingulum	-24	30	1	688	0.0002
L. Inferior Parietal Lobule	-24	-36	30	96	0.0007
R. Lingual Gyrus	12	-51	5	352	0.0009
R. Cerebellum	32	-71	-34	160	0.0013
B. Loss Cue – No Incentive Cue					
Comparison Subjects > MDD					
R. Cerebellum	20	-56	-17	96	0.0009
MDD > Comparison Subjects					
L Insula	-38	-7	-6	472	0.0000
R Medial Frontal Gyrus	2	30	40	224	0.0001
L Postcentral Gyrus	-40	-17	31	96	0.0003
Dorsal Anterior Cingulate	2	23	16	176	0.0011
R Posterior Cingulate	6	-20	41	96	0.0002
L Middle Temporal Gyrus	-34	-65	12	248	0.0001
L Lingual Gyrus	-28	-61	-1	296	0.0001

Note: x, y, and z correspond to the Talairach coordinates of the peak voxel. Talairach coordinates were computed from MNI space using the formula proposed by Brett and coworkers (S9).

Volume = Size of the region exceeding the statistical threshold ($p<0.005$); R= right; L=left.

TABLE S4. Regions Showing Group Differences Between MDD (n = 26) and Comparison Subjects (n = 31) In Response to Gains and Penalties

Region	*x*	*y*	*Z*	Volume (mm^3)	Peak Voxel p-value
A. Gain – No-Change Feedback					
Comparison Subjects > MDD					
R Caudate	14	15	11	320	0.0001†
	16	0	19	424	0.0005†
L Caudate	-12	-4	21	336	0.0004†
	-20	-27	19	104	0.0017
L Nucleus Accumbens*	-8	10	-8	64	0.0002
R Insula	32	17	2	120	0.0006
L Insula	-32	-4	20	128	0.0004
R Inferior Frontal Gyrus	50	24	24	160	0.0002
R Middle Frontal Gyrus	20	48	8	384	0.0001
	51	18	37	896	0.0001
	28	15	48	344	0.0001
R Medial Frontal Gyrus	4	47	30	216	0.0005
L Precentral Gyrus	-51	-3	31	264	0.0002
R Rostral Anterior Cingulate	6	29	9	280	0.0005
R Dorsal Anterior Cingulate	10	18	30	136	0.0006
L Posterior Cingulate	-2	-29	28	136	0.0003
R Middle Temporal Gyrus	51	-57	0	408	0.0002
L Cerebellum	-8	-62	-20	208	0.0002
	-16	-76	-24	160	0.0002
MDD > Comparison Subjects					
L Fusiform Gyrus	-40	-14	-25	456	0.00024
B. Penalty vs. No-Change Feedback					
Comparison Subjects > MDD					
R Caudate	14	23	11	296	0.0007
L Caudate	-8	-2	12	168	0.0005
L Thalamus	-18	-25	15	576	0.0001
R Inferior Frontal Gyrus	44	29	20	1472	0.0000
R Middle Frontal Gyrus	30	15	43	152	0.0007
L Precentral Gyrus	-53	-3	31	224	0.0004
L Posterior Cingulate	-2	-13	27	96	0.0012
R Superior Temporal Gyrus	50	10	-11	144	0.0001
R Middle Temporal Gyrus	67	-40	3	640	0.0000
L Middle Temporal Gyrus	-61	-51	7	128	0.0005
L Inferior Occipital Gyrus	-34	-81	-7	128	0.0003
MDD > Comparison Subjects					
L Precuneus	-16	-54	22	440	0.0000
R Cerebellum	30	-76	-26	168	0.0013

Note: x, y, and z correspond to the Talairach coordinates of the peak voxel. Talairach coordinates were computed from MNI space using the formula proposed by Brett and coworkers (S9). Volume = Size of the region exceeding the statistical threshold ($p<0.005$); R= right; L=left. *8 voxels, did not reach cluster size significance threshold. † Significant at $p < .05$ following correction for multiple comparisons with Monte Carlo simulation restricted to basal ganglia volume.

TABLE S5. Absolute and proportional volume (adjusted for total intracranial volume) for the four basal ganglia regions for MDD (n = 26) and Comparison (n = 31) subjects. Volumes are expressed in cubic millimeters.

	Comparison subjects		**MDD subjects**	
	Mean	SD	Mean	SD
Intracranial volume	1562421	191574	1520071	150388
Absolute volumes				
Left Caudate	3433	447	3427	507
Left_Putamen	5472	732	5550	697
Left_Pallidus	1718	252	1659	248
Left_NAcc	630	114	617	118
Right_Caudate	3592	520	3645	516
Right_Putamen	5369	717	5364	697
Right_Pallidus	1781	279	1658	287
Right_NAcc	548	74	560	128
Proportional volume				
Left_Caudate	0.00221	0.00025	0.00226	0.00027
Left_Putamen	0.00353	0.00044	0.00366	0.00037
Left_Pallidus	0.00111	0.00015	0.00109	0.00013
Left_NAcc	0.00041	0.00009	0.00041	0.00008
Right_Caudate	0.00231	0.00027	0.00240	0.00027
Right_Putamen	0.00346	0.00040	0.00354	0.00038
Right_Pallidus	0.00114	0.00015	0.00109	0.00016
Right_NAcc	0.00035	0.00006	0.00037	0.00007

NAcc = nucleus accumbens

Supplemental Material Figure Legends

FIGURE S1. Affective ratings during the monetary incentive delay task in MDD (N=30) and comparison (N=31) subjects. (**A**) Cue-related valence ratings; (**B**) cue-related arousal ratings; (**C**) outcome-related valence ratings; and (**D**) outcome-related arousal ratings collected during the task (averaged across the assessments occurring after blocks 2 and 4). Ratings were made using 5-point scales to evaluate affective response to the cues and outcomes with respect to valence (e.g., "*Please rate how you felt while waiting to push the button on a reward trial*"; 1=most negative feeling, 5=most positive feeling) and arousal (e.g., "*Please rate the strength of this feeling*"; 1=low intensity, 5=high intensity).

FIGURE S2. Secondary findings emerging from analyses investigating reward-related anticipatory activation in MDD (N=26) and comparison (N=31) subjects.
Relative to comparison subjects, the MDD group showed relatively higher activation to reward cues [Reward cue – No-incentive cue] in bilateral dorsolateral prefrontal cortex (PFC) (x=24, y=22, z=40 and x=-28, y=24, z=40). Follow-up analyses revealed group differences for reward cues ($p<0.009$) but not loss or no-incentive cues. L = Left.

FIGURE S3. Secondary findings emerging from analyses investigating reward-related consummatory activation in MDD (N=26) and comparison (N=31) subjects.
Relative to comparison subjects, the MDD group showed relatively lower activation to gain feedback [Gain feedback – No-change feedback] in the dorsal anterior cingulate cortex (x=10,

y=18, z=30). Follow-up analyses revealed group differences for reward feedback ($p<0.001$), but not penalty or no-change feedback. L = Left.

FIGURE S4. Secondary findings emerging from analyses investigating penalty-related anticipatory activation in MDD (N=26) and comparison (N=31) subjects.
Relative to comparison subjects, MDD subjects showed relatively higher activation to penalty cues [Loss cue – No-incentive cue] in the (**A**) left insula (x=-38, y=-7, z=-6), (**B**) right ventrolateral prefrontal cortex (PFC) (X=40, Y=44, Z=8), and (**C**) dorsal anterior cingulate cortex (ACC) (x=2, y=23, z=16). Follow-up analyses revealed that the insula finding was due to significantly lower activation to no-incentive cues in MDD relative to comparison subjects ($p<0.015$); for the right ventrolateral PFC and dorsal ACC regions, MDD subjects had significantly higher activation to both loss and reward cues ($p<0.05$). L = Left, A = Anterior.

FIGURE S5. Secondary findings emerging from analyses investigating penalty-related consummatory activation in MDD (N=26) and comparison (N=31) subjects.
Relative to comparison subjects, MDD subjects showed significantly lower relative activation to penalty feedback [Penalty Feedback – No-change feedback] in the (**A**) right caudate (x=14, y=23, z=11), and (**B**) left caudate (x=-8, y=-2, z=12). Follow-up analyses revealed that the right caudate finding was due to a trend for higher activation to no-incentive cues for MDD relative to comparison subjects ($p=0.074$); for the left caudate, follow-up analyses revealed that MDD subjects had decreased activation only to penalty feedback ($p<0.013$). L = Left.

FIGURE S6. Examples of the automated labeling of the caudate in four representative MDD participants. For each participant, images on the left display high-resolution coronal and axial slices cutting passing through the caudate; images on the right show the same slices with the left caudate highlighted in green are.

FIGURE S1

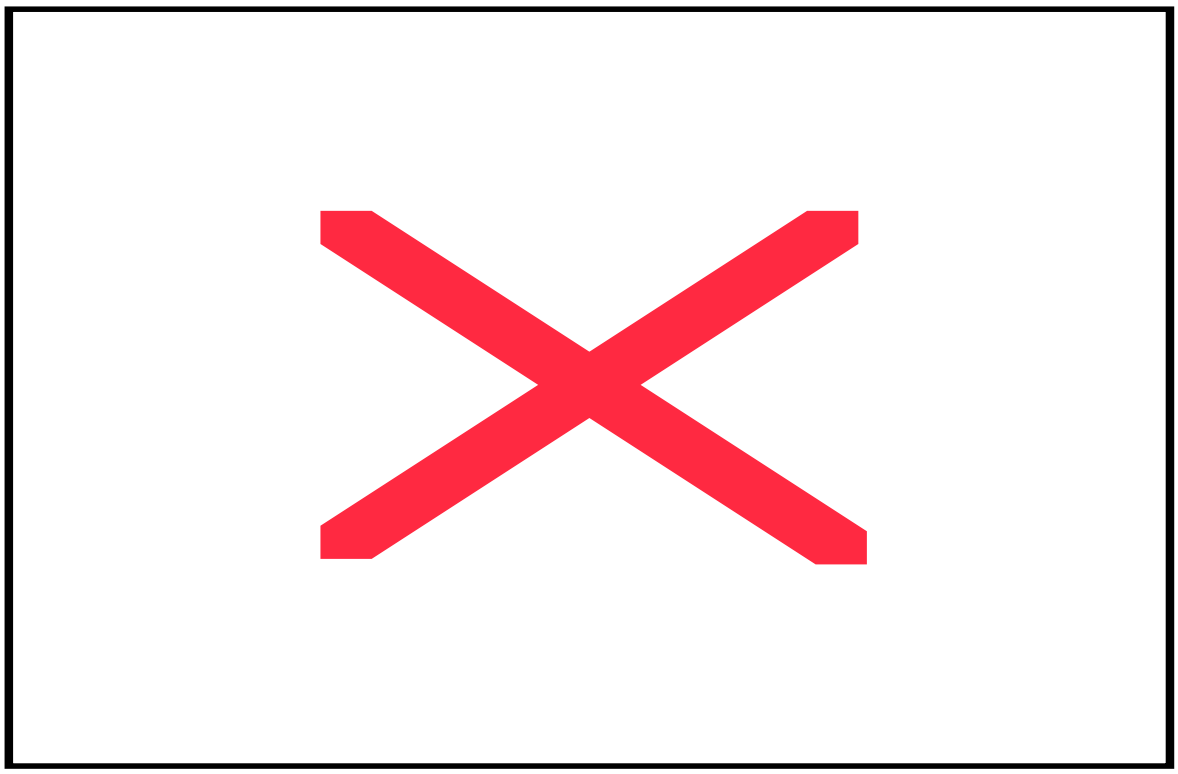

FIGURE S2

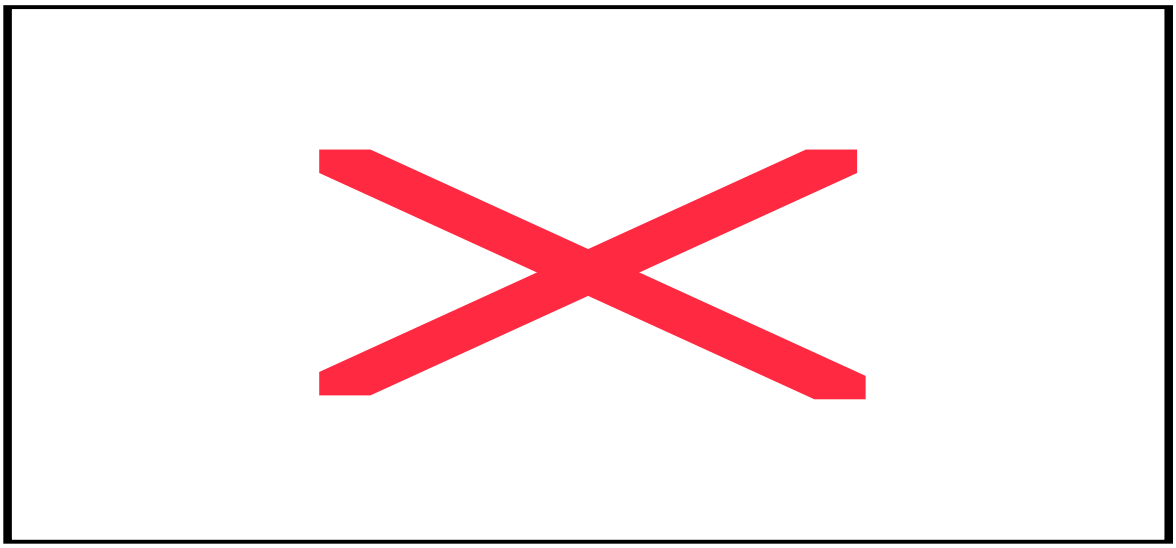

FIGURE S3

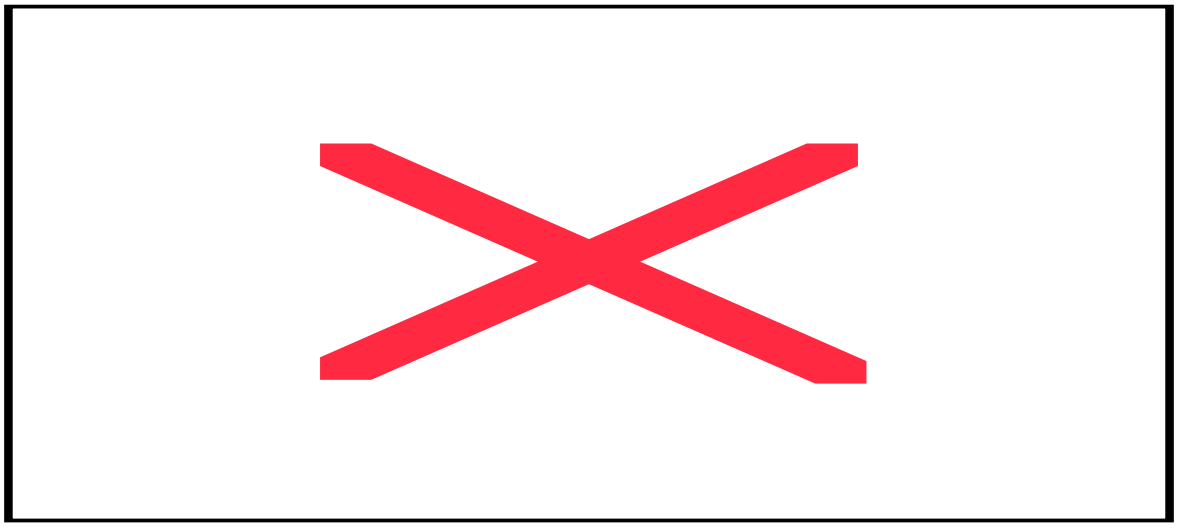

FIGURE S4

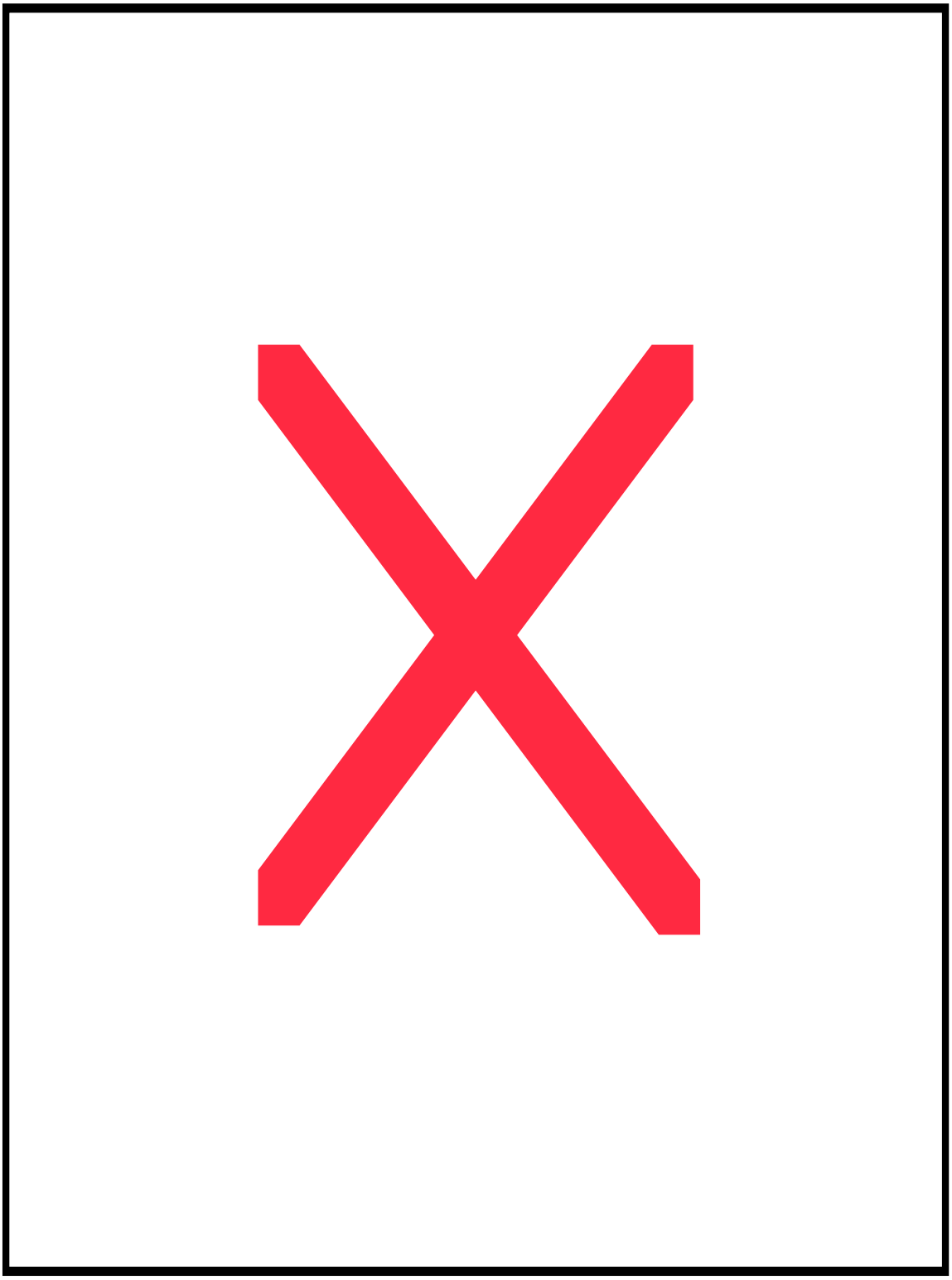

FIGURE S5

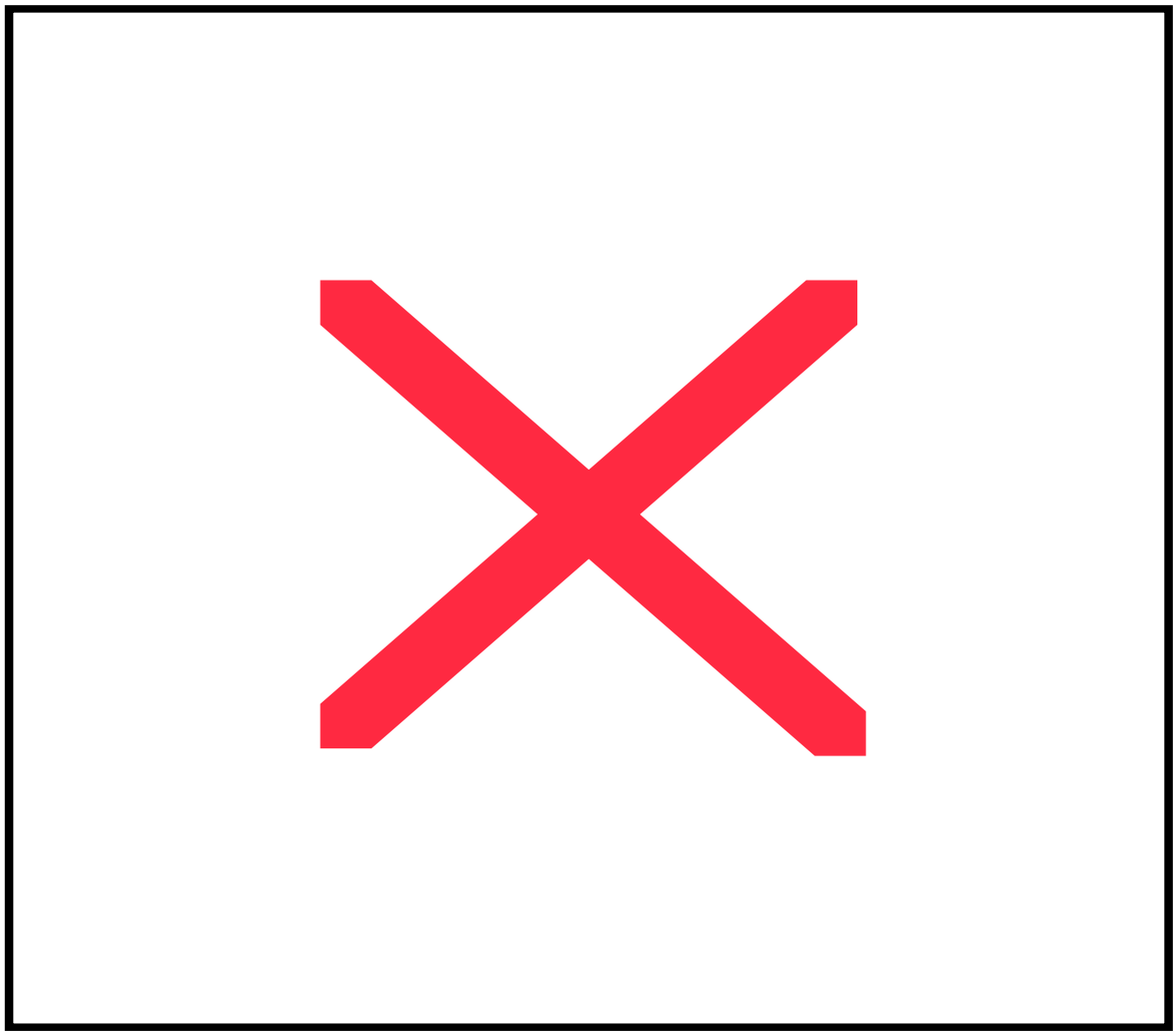

FIGURE S6